$(C_6H_{14}N_2)\{Zn[ZnB_2P_4O_{15}(OH)_2]\cdot(C_6H_{13}N_2)Cl\}$: A New Templated Zincoborophosphate

Ya-Xi Huang, Gerd Schäfer,† Wilder Carrillo-Cabrera, Horst Borrmann, Raul Cardoso Gil, and Rüdiger Kniep*

Max-Planck-Institut für Chemische Physik fester Stoffe, Nöthnitzer Str. 40, D-01187 Dresden, Germany

Received August 18, 2003. Revised Manuscript Received September 30, 2003

Colorless crystals of $(C_6H_{14}N_2)\{Zn[ZnB_2P_4O_{15}(OH)_2]\cdot(C_6H_{13}N_2)Cl\}$ **(1)** were prepared from mixtures of $ZnCl_2$, B_2O_3, diaza-bicyclo[2.2.2]octane (DABCO), and 85% H_3PO_4 under mild hydrothermal conditions (170 °C). The crystal structure was determined by single-crystal X-ray diffraction (monoclinic, $P2_1/c$ (No. 14), a = 1704.3(1) pm, b = 937.03(5) pm, c = 1619.75(8) pm, β = 96.894(3)°, Z = 2). The crystal structure contains tetrahedral zigzag ribbons, $^1_\infty\{[ZnB_2P_4O_{15}(OH)_2]^{4-}\}$, running along [010]. Additional ZnO_2NCl tetrahedra at the borders complete the ribbons by sharing common O-corners with the zincoborophosphate polymer. The nitrogen atoms of the quaternary ZnO_2NCl tetrahedra belong to monoprotonated $(HDABCO)^+$ ions. A second (diprotonated) species, $(H_2DABCO)^{2+}$, acts as a pure template and is fixed to adjacent zincoborophosphate ribbons along [100] via hydrogen bonds. The title compound **1** can be described as an adduct of $(C_6H_{14}N_2)\{Zn[ZnB_2P_4O_{15}(OH)_2]\}$ with diaza-bicyclo[2.2.2]octane-hydrochloride. Thermoanalytical and X-ray powder diffraction investigations to high temperatures (740 °C) show the decomposition of **1** and the formation of a $NH_4[ZnBP_2O_8]$ polymorph as an intermediate.

1. Introduction

Open-framework inorganic materials are of considerable interest due to their established or potential applications in sorption and separation, heterogeneous catalysis, and ion exchange.[1] Borophosphates as a relatively young research field have already shown a broad and interesting structural chemistry.[2] Several organo-templated borophosphates with open-framework structures are also known.[3] In our recent investigations on borophosphates using organic templates, we obtained the fluorine-substituted borophosphate $(C_2H_{10}N_2)[BPO_4F_2]$.[4] With respect to microporous and zeolite-analogous systems such as alumosilicates,[5] aluminum/alumophosphates,[6] and substituted variants,[7] gallium/gallo-,[8] and zincophosphates,[9] we have succeeded in characterizing new open-framework structures based on zincoborophosphates. With the syntheses of $A[ZnBP_2O_8]$ ($A = K^+, NH_4^+, Rb^+, Cs^+$) a new class of compounds with tetrahedral frameworks has been obtained, with topologies that display a close relationship to alumosilicates (the feldspar family and Gismondine).[10] A chiral zincoborophosphate, $Na[ZnBP_2O_8]\cdot H_2O$,[11] with close structure relations to the CZP topology[12] is formed by dehydration of the Na−Zn-phase of the isostructural series $M^IM^{II}(H_2O)_2[BP_2O_8]\cdot yH_2O$ (M^I: Li, Na, K; M^{II}: Mn, Fe, Co, Ni, Zn; y: 0.5, 1)[13] which contains helical ribbons of corner-linked borate and phosphate tetrahedra. No organo-templated zincoborophosphate was reported up to now, although many efforts were directed to the syntheses of zincoborophosphates.[14] Here, we report on the first example of an organo-templated zincoborophosphate: $(C_6H_{14}N_2)\{Zn[ZnB_2P_4O_{15}(OH)_2]\cdot(C_6H_{13}N_2)Cl\}$ **(1)**.

* To whom correspondence should be addressed. Tel: 49 ((0)351)-4646-3000. Fax: 49 ((0)351)-4646-3002. E-mail:kniep@cpfs.mpg.de.
† Present address: Institut für Neue Materialien, Saarbrücken, Germany.

(1) Cheetham, A. K.; Férey, G.; Loiseau, T. *Angew. Chem., Int. Ed.* **1999**, *38*, 3268.
(2) Kniep, R.; Engelhardt, H.; Hauf, C. *Chem. Mater.* **1998**, *10*, 2930.
(3) (a) Sevov, S. C. *Angew. Chem., Int. Ed. Engl.* **1996**, *35*, 2630. (b) Kniep, R.; Schäfer, G. *Z. Anorg. Allg. Chem.* **2000**, *626*, 141. (c) Schäfer, G.; Borrmann, H.; Kniep, R. *Z. Anorg. Allg. Chem.* **2001**, *627*, 61. (d) Schäfer, G.; Carrillo-Cabrera, W.; Leoni, S.; Borrmann, H.; Kniep R. *Z. Anorg. Allg. Chem.* **2002**, *628*, 67. (e) Bontchev, R. P.; Do, J.; Jacobson, A. J. *Inorg. Chem.* **2000**, *39*, 3320 and references therein.
(4) Huang, Y.-X.; Schäfer, G.; Borrmann, H.; Zhao, J.-T.; Kniep, R. *Z. Anorg. Allg. Chem.* **2002**, *629*, 3.
(5) Breck, D. W. *Zeolite Molecular Sieves*; Wiley: New York, 1974.
(6) (a) Wilson, S. T.; Lok, B. M.; Messina, C. A.; Cannan, T. R.; Flanigen, E. M. *J. Am. Chem. Soc.* **1982**, *104*, 1146. (b) Flanigen, E. M.; Lok, B. M.; Patton, R. L.; Wilson, S. T. *Pure Appl. Chem.* **1986**, *58*, 1351.
(7) (a) Feng, P.; Bu, X.; Stucky, G. D. *Nature* **1997**, *388*, 735. (b) Hartmann, M.; Kevan, L. *Chem. Rev.* **1999**, *99*, 9(3), 635.
(8) (a) Estermann, M.; McCusker, L. B.; Baerlocher, C.; Merrouche, A.; Kessler, H. *Nature* **1991**, *352*, 320. (b) Loiseau, T.; Férey, G. *J. Solid State Chem.* **1994**, *111*, 403.
(9) (a) Bedard, R. L. UOP Inc. USA, U.S. Patent 005302362, 1994 [*Chem. Abstr.* **1994**, *121*, 208502q]. (b) Harrison, W. T. A.; Hannooman, L. *Angew. Chem., Int. Ed. Engl.* **1997**, *36*, 640. (c) Harmon, S. B.; Sevov, S. C. *Chem. Mater.* **1998**, *10*, 3020.
(10) (a) Kniep, R.; Schäfer, G.; Engelhardt, H.; Boy, I. *Angew. Chem., Int. Ed.* **1999**, *38*, 3641. (b) Kniep, R.; Schäfer, G.; Borrmann, H. *Z. Kristallogr. NCS* **2000**, *215*, 335.
(11) Boy, I.; Stowasser, F.; Schäfer, G.; Kniep, R. *Chem. Eur. J.* **2001**, *7*, 834.
(12) Meier, W. M.; Olson, D. H.; Baerlocher, C. *Atlas of Zeolite Structure Types*, 4th ed.; Elsevier: London, 1996; p 108.
(13) Kniep, R.; Will, H. G.; Boy, I.; Röhr, C. *Angew. Chem., Int. Ed. Engl.* **1997**, *36*, 1013.
(14) Wiebcke, M. *J. Mater. Chem.* **2002**, *12*, 143.

10.1021/cm0311224 CCC: $25.00
Published on Web 11/27/2003

Table 1. Crystallographic Data and Refinement Results of 1, esd's Are Given in the Parentheses

molecular formula	$(C_6H_{14}N_2)\{Zn[ZnB_2P_4O_{15}(OH)_2]\cdot(C_6H_{13}N_2)Cl\}$
space group	$P2_1/c$ (No. 14)
a (pm)	1704.3(1)
b (pm)	937.03(5)
c (pm)	1619.75(8)
β (°)	96.894(3)
V (10^6·pm^3)/Z	2567.9(2)/2
ρ_{calc} (g·cm^{-3})	2.103
diffractometer	Rigaku AFC7 CCD, Mo Kα radiation, graphite monochromator
μ (Mo Kα) (mm^{-1})	2.311
scan type	ϕ/ω
2θ range (deg)	4.82−60.8
temperature (K)	295
Miller-index range	$-15 \le h \le 22$, $-9 \le k \le 12$, $-22 \le l \le 21$
total data collected/unique data	20609/6484
observed data ($I > 2\sigma(I)$)/R_{int}/R_σ	5316/0.0468/0.0597
no. of parameters refined	466
R1 ($F_o > 4\sigma(F_o)$)/R1 (all data)	0.0640/0.0879
wR2 ($F_o > 4\sigma(F_o)$)/wR2 (all data)	0.1153/0.1229
goodness-of-fit (for F^2)	1.149
residual electron density (max/min) (e × 10^{-6} pm^{-3})	2.035/−0.696[a]

[a] The positive residual electron density close to the O15.

2. Experimental Section

Syntheses and Characterization. 1 was prepared under mild hydrothermal conditions from a mixture of 3.894 g (28.6 mmol) of $ZnCl_2$ (Alfa, 99%), 0.994 g (14.3 mmol) of B_2O_3 (Alfa, 99.9%), 6.41 g (57.2 mmol) of diaza-bicyclo[2.2.2]-octane (DABCO, Aldrich, 99%), 7 mL of 85% H_3PO_4 (Merck, p.a.), 10 mL of deionized water and with stirring at 100 °C. The highly viscous white gel with a pH value of 1.5−2.0 was filled into a Teflon autoclave (Roth Bola, V = 20 mL, degree of filling ≈ 60%) and held at 170 °C for 3 days under autogenous pressure. Colorless platy crystals of **1** were separated by filtration, washed with deionized water, and dried at 60 °C in air. The Zn^{2+} source, the pH value, and the degree of filling cause a significant influence on the reaction products formed. When $ZnCl_2$ is replaced by ZnO but the same reaction conditions are applied, the reaction product consists of the known compound, $Zn_3(C_6H_{14}N_2)_3[B_6P_{12}O_{39}(OH)_{12}]\cdot(C_6H_{14}N_2)[HPO_4]$ (**2**), which was already reported only recently.[3d] In the preparation of **1**, when the degree of filling is lower or equal to 50% but all other conditions are kept constant, **2** and another "zinc-borophosphate" with a molar ratio of Zn:B:P:C:N = 2:2:5:12:4[15] are obtained. At a pH value of 2.5−3, $(C_6H_{14}N_2)[Zn_2(HPO_4)_3]$[16] and the "zinc-borophosphate" already mentioned[15] are formed as the reaction products.

Phase purity of **1** was controlled using X-ray powder diffraction (Huber Image Foil Guinier Camera G670, Cu $K\alpha_1$ radiation, Ge monochromator). Zn, B, and P contents were analyzed using ICP-AES (Varian Vista, radial observation), while a hot extraction method was applied for organic carbon and nitrogen (Leco CHNS-932), (obs.(esd)/calc.) mass %: Zn 16.76(6)/16.08; B 2.62(4)/2.66; P 15.0(1)/15.24; C 17.82(2)/17.73; N 6.99(2)/6.89. The good agreement of observed and calculated values confirms the given chemical formula (**1**). The presence of Cl was confirmed by EDX measurements (Philips XL 30 with software package EDAX, sample sputtered with carbon).

(15) Huang, Y.-X.; Kniep R. Unpublished results.
(16) Harrison, W. T. A.; Martin T. E.; Gier, T. E.; Stucky, G. D. *J. Mater. Chem.* **1992**, *2*, 175.

Table 2. Atomic Coordinates and Equivalent/Isotropic Displacement Parameters (10^{-4} pm^2) in the Crystal Structure of 1; esd's Are Given in the Parentheses

atom	x	y	z	U_{eq}/U_{iso}[a]
Zn1	0.39151(3)	0.92506(6)	0.19288(3)	0.01641(13)
Zn2	0.09638(3)	0.24598(6)	0.25098(3)	0.01408(12)
Cl1	0.06668(9)	0.25843(16)	0.38120(8)	0.0316(3)
P1	0.53837(7)	0.15744(13)	0.19843(7)	0.0150(2)
P2	0.20015(8)	0.45220(13)	0.16002(8)	0.0161(2)
P3	0.20960(7)	0.01202(13)	0.17821(8)	0.0159(2)
P4	0.34474(8)	0.72419(14)	0.04696(8)	0.0201(3)
B1	0.2299(3)	0.7330(5)	0.1429(3)	0.0133(10)
B2	0.3403(4)	0.9204(6)	0.1856(4)	0.0197(11)
O1	0.3963(2)	0.8466(4)	0.0801(2)	0.0206(7)
O2	0.1830(2)	0.8549(3)	0.1617(2)	0.0205(7)
O3	0.2906(2)	0.4525(4)	0.1901(2)	0.0243(8)
O4	0.4558(2)	0.1006(4)	0.1890(3)	0.0281(9)
O5	0.2561(2)	0.7577(4)	0.0562(2)	0.0214(7)
O6	0.2983(2)	0.7092(3)	0.2000(2)	0.0167(7)
O7	0.17683(2)	0.6088(3)	0.1338(2)	0.0194(7)
O8	0.4545(2)	0.8119(3)	0.2772(2)	0.0194(7)
O9	0.2947(2)	0.0199(4)	0.2147(2)	0.0250(8)
O10	0.1816(2)	0.3540(4)	0.0875(2)	0.0279(9)
O11	0.1966(3)	0.0840(4)	0.0916(3)	0.0298(10)
O12	0.3647(2)	0.5853(4)	0.0984(3)	0.0319(9)
O13	0.1552(2)	0.0741(4)	0.2354(2)	0.0239(8)
O14	0.1575(2)	0.4134(4)	0.2340(2)	0.0249(8)
O15	0.5896(3)	0.0571(4)	0.2604(3)	0.0490(14)
O16	0.5709(4)	0.1356(5)	0.1137(3)	0.0574(16)
O17	0.3516(3)	0.6864(5)	0.9576(2)	0.0416(12)
N1	0.3592(3)	0.6165(5)	0.9556(3)	0.0304(11)
N2	0.6340(3)	0.8606(5)	0.0991(3)	0.0254(10)
N3	0.8678(3)	0.2487(5)	0.0659(3)	0.0240(9)
N4	0.9939(2)	0.2459(4)	0.1657(2)	0.0161(8)
C1	0.2784(4)	0.6630(7)	0.9214(4)	0.0358(15)
C2	0.5998(4)	0.7591(7)	0.1565(4)	0.0369(15)
C3	0.7179(4)	0.8248(8)	0.0935(5)	0.0403(16)
C4	0.4108(4)	0.6176(7)	0.8864(5)	0.0401(15)
C5	0.5873(5)	0.8529(7)	0.0146(4)	0.0402(16)
C6	0.0245(4)	0.7113(8)	0.3924(5)	0.0426(17)
C7	0.0952(5)	0.1503(11)	0.0005(5)	0.063(3)
C8	0.9258(5)	0.1539(11)	0.0322(5)	0.058(2)
C9	0.9757(5)	0.3888(9)	0.1346(7)	0.076(3)
C10	0.8985(6)	0.3947(9)	0.0767(8)	0.089(4)
C11	0.9269(4)	0.1961(14)	0.2055(5)	0.075(4)
C12	0.8508(5)	0.1914(16)	0.1460(5)	0.086(4)
H1	0.196(5)	0.150(8)	0.094(5)	0.05*
H2	0.593(4)	0.219(8)	0.092(4)	0.05*
H3	0.638(4)	0.531(8)	0.033(4)	0.05*
H4	0.627(4)	0.945(8)	0.121(4)	0.05*
H5	0.823(4)	0.253(7)	0.031(4)	0.05*
H6	0.754(4)	0.648(8)	0.039(5)	0.05*
H7	0.731(4)	0.602(8)	0.126(5)	0.05*
H8	0.555(5)	0.796(8)	0.168(5)	0.05*
H9	0.638(4)	0.765(7)	0.207(5)	0.05*
H10	0.742(4)	0.835(8)	0.143(5)	0.05*
H11	0.732(4)	0.871(8)	0.042(5)	0.05*
H12	0.537(4)	0.613(8)	0.085(4)	0.05*
H13	0.608(4)	0.517(8)	0.151(4)	0.05*
H14	0.525(4)	0.859(8)	0.032(4)	0.05*
H15	0.604(4)	0.926(8)	−0.022(4)	0.05*
H16	0.565(4)	0.662(8)	0.945(4)	0.05*
H17	0.645(4)	0.736(8)	0.940(5)	0.05*
H18	0.017(4)	0.053(8)	0.121(4)	0.05*
H19	0.049(5)	0.199(8)	0.072(4)	0.05*
H20	0.896(4)	0.074(8)	0.065(5)	0.05*
H21	0.927(4)	0.180(8)	−0.028(5)	0.05*
H22	1.023(5)	0.404(9)	0.114(5)	0.05*
H23	0.990(5)	0.458(8)	0.151(5)	0.05*
H24	0.875(5)	0.459(8)	0.061(5)	0.05*
H25	0.924(5)	0.356(8)	0.025(5)	0.05*
H26	0.930(5)	0.298(8)	0.227(5)	0.05*
H27	0.925(5)	0.173(8)	0.246(5)	0.05*
H28	0.813(5)	0.174(9)	0.156(5)	0.05*
H29	0.836(5)	0.306(8)	0.150(5)	0.05*

[a] Asterisk (*) indicates refined with isotropic displacement parameters.

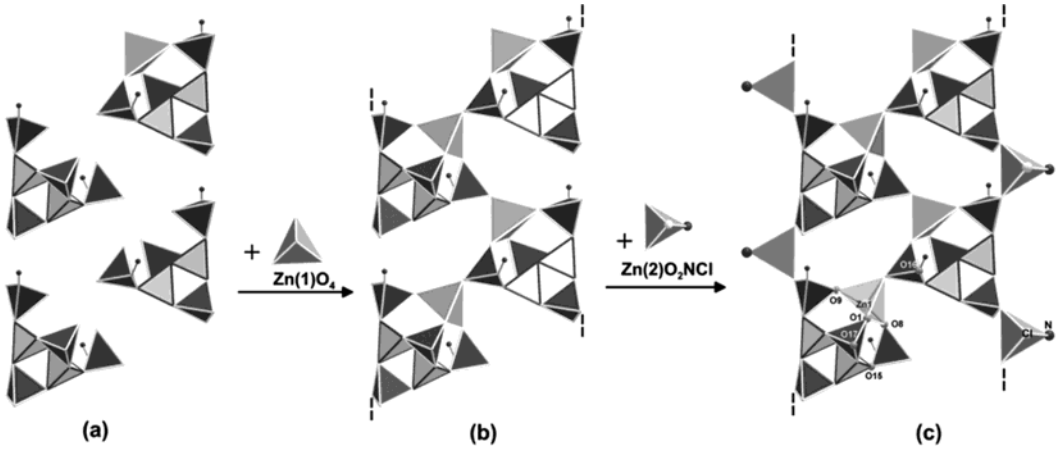

Figure 1. Scheme showing loop-branched oligomers $[B_2P_4O_{15}(OH)_2]^{6-}$ (a) together with ZnO_4 tetrahedra that form into zigzag zincoborophosphate ribbons running along [010] (b); ZnO_2NCl tetrahedra close the zigzag zincoborophosphate ribbons and complete eight-membered tetrahedral rings within the ribbons (c). PO_4 tetrahedra: dark gray; BO_4 tetrahedra: light gray; ZnO_4 and ZnO_2-NCl tetrahedra: medium gray. Cl atoms: light gray sphere; N atoms: dark gray sphere.

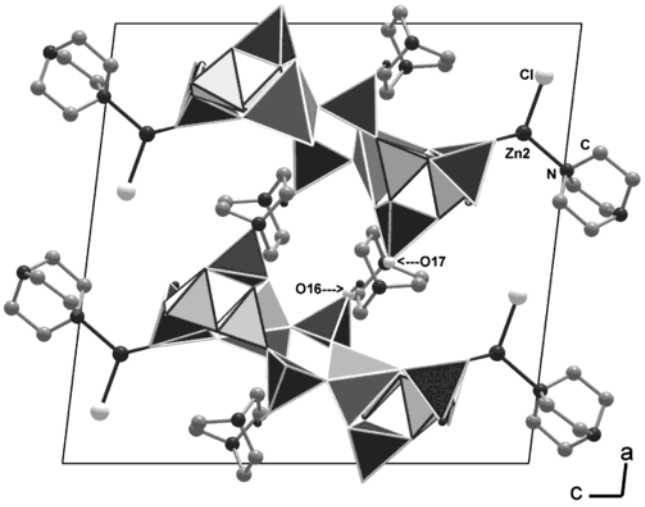

Figure 2. Crystal structure of **1** viewed along [010] shows ribbons parallel stacking along [100]. The $(H_2DABCO)^{2+}$ ions are located between adjacent eight-membered rings of neighboring ribbons along [100]; O16 and O17 are denoted for the very short distance between two neighboring ribbons. PO_4 tetrahedra: dark gray; BO_4 tetrahedra: light gray; ZnO_4 and ZnO_2NCl tetrahedra: medium gray. Cl atom: light gray sphere; N atom: dark gray sphere. DABCO protons are omitted for clarity.

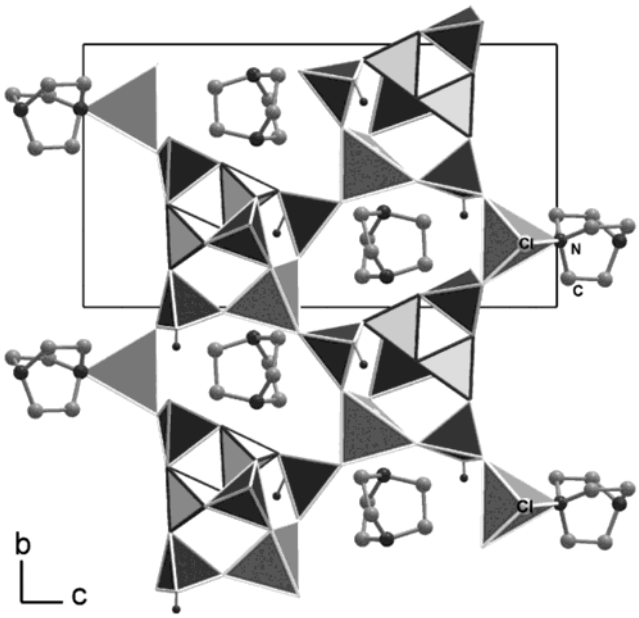

Figure 3. Crystal structure of **1** viewed along [100] shows a ribbon running along [010]. PO_4 tetrahedra: dark gray; BO_4 tetrahedra: light gray; ZnO_4 and ZnO_2NCl tetrahedra: medium gray. Cl atoms: light gray sphere; N atoms: dark gray sphere. DABCO protons are omitted for clarity.

Differential thermal analysis and thermogravimetry (DTA/TG) were carried out in a static air atmosphere with heating and cooling rates of 5 °C/min (Netzsch STA 409).

HT-XRD investigations were carried out on a high-temperature X-ray powder diffractometer (STOE STADI-MP, Cu $K\alpha_1$ radiation, Ge monochromator, high-temperature attachment of STOE) by filling a powdered sample of **1** in an open-quartz capillary of 0.5-mm diameter. The X-ray diffraction powder patterns were collected in the temperature range 23−740 °C with 1 h of scanning time per step. The heating rate between the temperature steps was 5 °C/min.

Crystal Structure Determination. A suitable but rather small single crystal of **1** (platelet, 0.04 × 0.03 × 0.02 mm^3) was fixed on a glass fiber with two-component glue. X-ray data were collected at 295 K using a Rigaku AFC7 four-circle diffractometer, equipped with a Mercury-CCD detector (Mo Kα radiation, graphite monochromator) in the angular range 4.8° ≤ 2θ ≤ 60.8° (240°-ϕ-scan, 60°-ω-scan at χ = 90°, 0.5° steps with 60-s exposure time per step, detector distance: 40 mm; 2θ -offset: −15°). The data were corrected for Lorentz and polarization effects. A numerical absorption correction was applied. The structure was solved in the space group $P2_1/c$ (No. 14) by direct methods using the program SHELXS-97-2.[17] Fourier calculations and subsequent full-matrix least-squares refinements were carried out using SHELXL-97-2[18] and applying neutral-atom scattering factors. The relative high positive residual density (of 2.035 e × 10^{-6} pm^{-3}) close to O15 is due to partial disordering effects, which could not be completely modeled. The crystallographic data are summarized in Table 1. After anisotropic displacement parameters had been included in the refinement, all hydrogen atoms could be located from difference Fourier maps. Atomic coordinates for **1** are given in Table 2.

The relative high equivalent displacement parameters of O15, O16, and O17 and of all the carbon atoms of the (DABCO) units might indicate a possible disordering of this part of the structure. However, various models, for example, with split positions or in a lower space group, did not result in decisive

(17) Sheldrick, G. M. *SHELXS 97-2, Program for the Solution of Crystal Structures*; University of Göttingen: Göttingen, 1997.

(18) Sheldrick, G. M. *SHELXL 97-2, Program for Crystal Structure Refinement*; University of Göttingen: Göttingen, 1997.

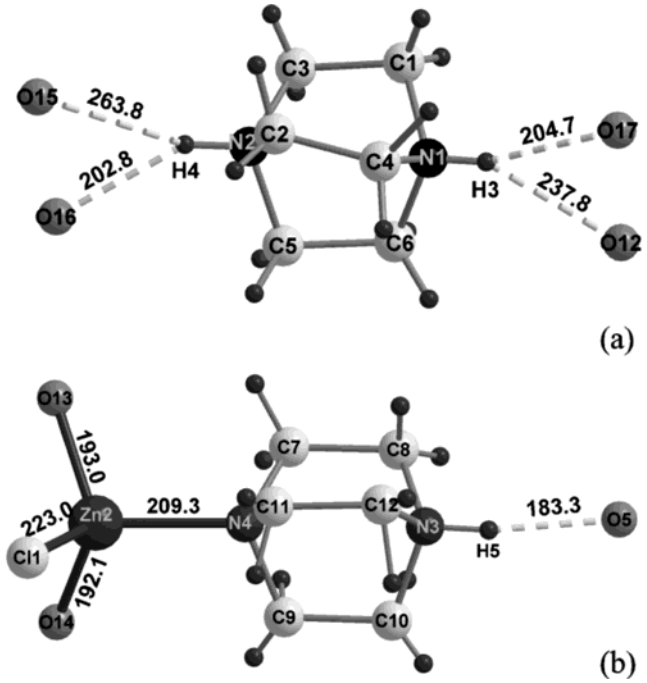

Figure 4. Hydrogen bonds N−H···O and the coordination of (a) $(H_2DABCO)^{2+}$ ions and (b) $ZnO_2Cl(HDABCO)^+$ groups.

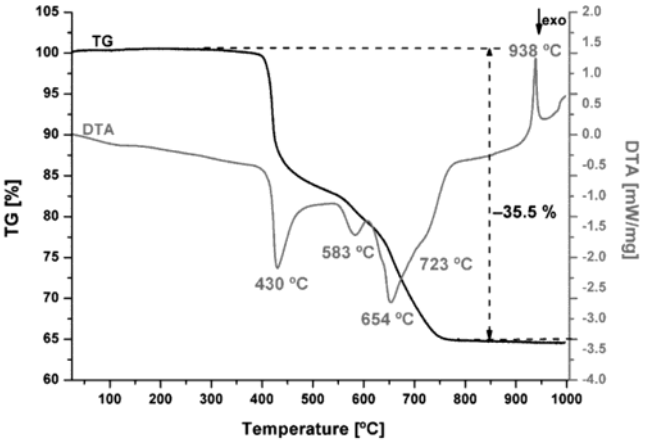

Figure 5. DTA/TG curves of **1**. For measurement details, see text.

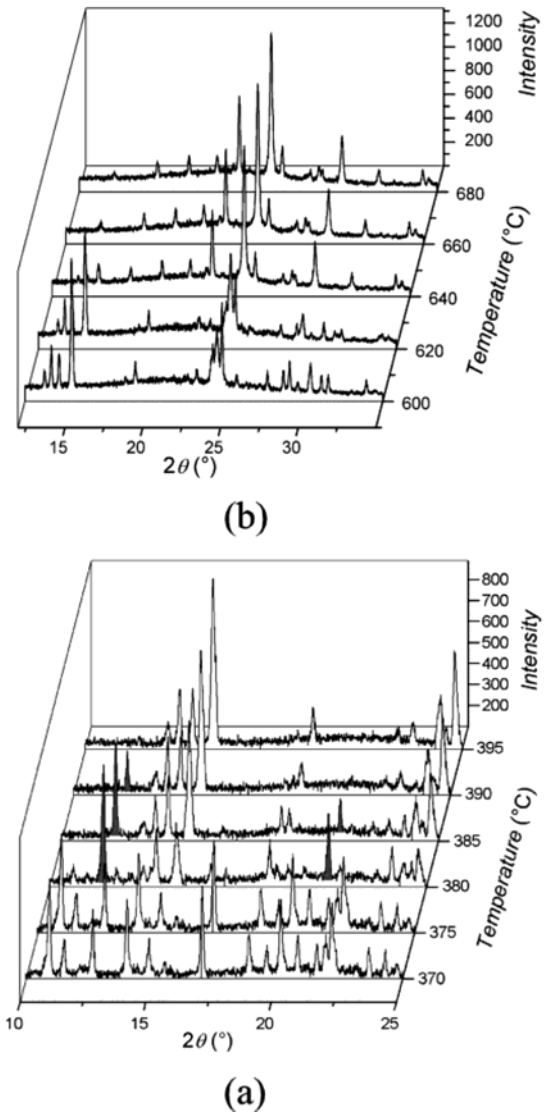

Figure 6. Selected high-temperature X-ray diffraction powder patterns during the decomposition of **1**, with (a) a temperature range from 370 to 395 °C and (b) a temperature range from 600 to 680 °C, Cu $K\alpha_1$ radiation. Reflections of the intermediate unidentified phase are marked in gray (b).

improvements of the refinement, resulting in similar residual electron density.

3. Results and Discussion

Crystal Structure Description. The borophosphate partial structure of **1** contains loop-branched oligomers, $[B_2P_4O_{15}(OH)_2]^{6-}$ (Figure 1a), consisting of two BO_4, two $(OH)PO_3$, and two PO_4 tetrahedra sharing common O-corners. Neighboring borophosphate oligomers are interconnected by $Zn1O_4$ tetrahedra sharing common O-corners with four adjacent phosphate groups. This results in tetrahedral zincoborophosphate zigzag ribbons, $^1_\infty\{[ZnB_2P_4O_{15}(OH)_2]^{4-}\}$ (Figure 1b), running along [010]. The terminal phosphate groups at the borders of the zincoborophosphate ribbons are bridged by Zn2-coordination-tetrahedra, ZnO_2NCl, which complete eight-membered tetrahedral rings within the ribbons (Figure 1c).

Figure 2 shows the crystal structure of **1** viewed along the *b* axis. The zincoborophosphate zigzag ribbons run parallel to each other along [100]. The distance between two neighboring ribbons along [100] is very short (249.5 pm ($d_{O16-O17}$)) compared with the size of DABCO ($d_{N\cdots N}$ = 252 pm). Therefore, the diprotonated $(H_2DABCO)^{2+}$ ions are located within the cavities between adjacent eight-membered rings of neighboring ribbons and are fixed via N−H···O hydrogen bonds (Figure 4a).

Figure 3 shows the ribbon viewing along [100]. The terminal $(HDABCO)^+$ groups connect adjacent ribbons via N−H···O hydrogen bonds (Figure 4b). The central part of the ribbons consists of a chain of PO_4- and ZnO_4-tetrahedra sharing common O-corners. This connection seems to be rather strong and rigid. The bulky $ZnO_2Cl(C_6H_{13}N_2)$ groups at the borders close the eight-membered rings by sharing common oxygen positions with two PO_4 tetrahedra. Due to the rigid connection of the central tetrahedral chain together with the bulky and flexible $ZnO_2Cl(HDABCO)^+$ groups at the borders of the ribbons, the O15 position has large displacement

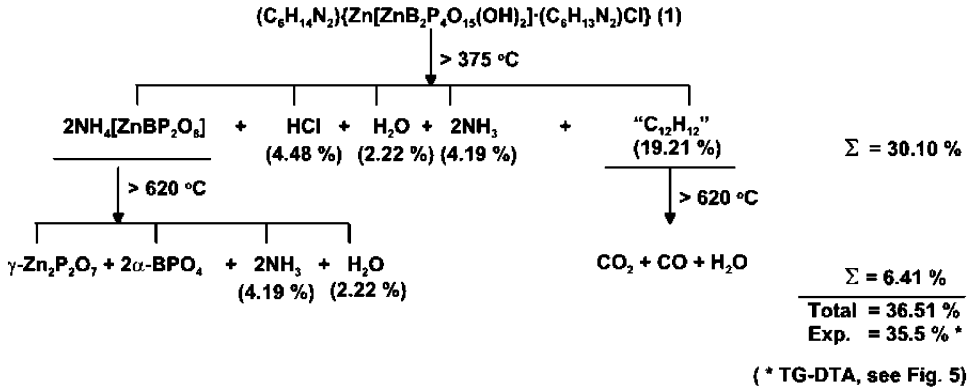

Figure 7. Scheme of the decomposition process of **1** during heating in the air according to high-temperature X-ray powder diffraction. The decomposition species contents are calculated according to the molar mass of **1**.

parameters and shows a high residual electron density close to it.

The PO_4 and $(OH)PO_3$ groups have an almost ideal tetrahedral geometry: $d_{P-O} = 149.5(4)-156.7(4)$ pm and $\angle O-P-O = 104.5(2)-114.6°$ (average bond length and angle: 153.13 pm and 109.4°). Both borate tetrahedra are severely distorted. The distances B1−O5 (154.1(6) pm) and B2−O5 (152.2(7) pm) are rather large compared with other borophosphates,[3,10−13] but the average B−O bond lengths (146.88 pm for B1 and 146.08 pm for B2, respectively) are still in the typical range for B−O distances with boron in tetrahedral coordination. Zn1 has a distorted tetrahedral coordination: $d_{Zn1-O} = 194.4(4)-198.2(4)$ pm, $\angle O-Zn1-O = 96.39(16)-122.01(16)°$, respectively, with the central Zn1 position shifted toward the face formed by O1, O8, and O9. Zn2 is tetrahedrally coordinated by two O atoms from the phosphate groups, one nonprotonated N atom of $(HDABCO)^+$ and one Cl atom with common distances and angles: $d_{Zn2-N} = 209.3(4)$ pm, $d_{Zn2-Cl} = 223.04(13)$ pm, $\angle O(N, Cl)-Zn2-O(N, Cl) = 106.36(12)-111.31(16)°$. Ternary zinc tetrahedra in zincophosphates are already known with ZnO_3Cl[19] or ZnO_3N.[20] **1** is the first example containing a quaternary Zn-tetrahedron, ZnO_2NCl, and can formally be described as an adduct of $(C_6H_{14}N_2)Zn[ZnB_2P_4O_{15}(OH)_2]$ with diaza-bicyclo[2.2.2]octane-hydrochloride.

Hydrogen bonds in the crystal structure of **1** can be classified as three different types of connections: one intra-ribbon and two types of inter-ribbons. In more detail, (a) *intra*-ribbon (within a single ribbon): O11−H1···O10 ($d_{O11\cdots O10}$ = 254.3 pm, ∠O11−H1···O10 = 170.41°); (b) *inter*-ribbon (linking adjacent ribbons along [100]): O16−H2···O17 ($d_{O16\cdots O17}$ = 249.5 pm, ∠O16−H2···O17 = 159.07°), N1−H3···O17 ($d_{N1\cdots O17}$ = 284.2 pm, ∠N1−H3···O17 = 161.41°), N1−H3···O12 ($d_{N1\cdots O12}$ = 249.5 pm, ∠N1−H3···O12 = 159.07°), N2−H4···O15 ($d_{N2\cdots O15}$ = 298.0 pm, ∠N2−H4···O15 = 130.37°), and N2−H4···O16 ($d_{N2\cdots O16}$ = 284.2 pm, ∠N2−H4···O16 = 148.41°); (c) *inter*-ribbon (linking adjacent ribbons in the (011)-plane): N3−H5···O5 ($d_{N3\cdots O5}$ = 271.6 pm, ∠N3−H5···O5 = 167.66°). Some hydrogen bond lengths are given in Figure 4.

Thermoanalyses and Identification of Intermediate Phases. The TG curve (Figure 5) during the decomposition of **1** shows a three-step reaction with an overall mass loss of 35.5% (36.5% calc., according to a hypothetical weight loss of 2 × $C_6H_{12}N_2$, 1 × HCl, and 2 × H_2O per formula unit), associated with three exothermic peaks in the DTA curve with maximum temperatures at 430, 583, and 654 °C, respectively, and a shoulder at 723 °C.

Some selected X-ray powder patterns (370−395 °C) are presented in Figure 6a and show that **1** is stable up to 375 °C, although the intensity of reflections decreases. At 380 °C **1** decomposes to a $NH_4[ZnBP_2O_8]$ polymorph[10] and an unidentified intermediate compound stable only between 380 and 390 °C (see some marked reflections in gray color in Figure 6a).

Figure 6b shows the continuous decomposition reaction in higher temperatures: $NH_4[ZnBP_2O_8]$ decomposes to a mixture of γ-$Zn_2P_2O_7$ (PDF database: 39-711) and α-BPO_4 (PDF database: 34-132) above 620 °C. After the sample is heated up to 1000 °C and cooled down to room temperature, the X-ray powder diffraction pattern of the resulting solid product showed it consisted of α-$Zn_2P_2O_7$ and α-BPO_4 (PDF files no. 8-238 and 34-132, respectively).

Figure 7 summarizes the results of the thermoanalytical and X-ray investigations. The scheme shows that the large amount of weight loss happened around 375 °C and the remaining weight loss was around 620 °C, which are according to the first step and the third step in the TG curve (Figure 5), respectively. Compared with the DTA/TG results, the higher weight loss of the first step (30.10%) and the lower weight loss of the third step (6.41%) are due to amorphous organic decomposition products remaining in the TG crucible at the first step, followed by complete oxidation at higher temperatures.

4. Conclusion

$Zn_3(C_6H_{14}N_2)_3[B_6P_{12}O_{39}(OH)_{12}]\cdot(C_6H_{14}N_2)[HPO_4]$[3d] (**2**) was the only borophosphate known up to now containing Zn and protonated DABCO templates. The crystal structure is completely different from that of the title compound and contains helical chains constructed from mixed octahedral−tetrahedral secondary building units, $^1_\infty\{Zn_3B_6P_{12}O_{39}(OH)_{12}]^{6-}\}$ (zinc in octahedral coordination) which are arranged around 3_1 screw axes. Two types of diprotonated $(H_2DABCO)^{2+}$ templates per formula unit interconnect the helical chains via N−H···O hydrogen bonds. Besides $(H_2DABCO)^{2+}$-tem-

(19) (a) Neeraj, S.; Natarajan, S. *J. Mater. Chem.* **2000**, *10*, 1171. (b) Yu, J.; Wang, Y.; Shi, Z.; Xu, R. *Chem. Mater.* **2001**, *13*, 2972.

(20) Harrison, W. T. A.; Nenoff, T. M.; Eddy, M. M.; Martin, T. E.; Stucky, G. D. *J. Mater. Chem.* **1992**, *2*, 1127.

plates, the title compound also contains monoprotonated $(HDABCO)^+$, which are bound to Zn(2) at the borders of the ribbons via a Zn−N bond. The introduction of the bulky $(HDABCO)^+$ together with Cl^- as coordinating ligands to the tetrahedral polymer causes significant structural peculiarities which favor the formation of ribbonlike zincoborophosphate arranged units.

Our continuing investigations in the Zn-borophosphate-DABCO system already show that further templated intermediates can be prepared. All of them are obtained via a mild hydrothermal route under acid conditions with only small changes in the synthesis parameters leading to different compositions as the main reaction product.

The structure determination of the $NH_4[ZnBP_2O_8]$-polymorph, which is obtained as an intermediate phase during thermal decomposition of the title compound, is in progress.

Acknowledgment. This work was supported by the Fonds der Chemischen Industrie (Frankfurt/Main). The authors would like to thank Anja Völzke and Birgit Kie*β*ler for chemical analyses, Susann Müller for DTA/TG, and Petra Scheppan for EDX investigations.

Supporting Information Available: CIF file for compound **1**. This material is available free of charge via the Internet at http://pubs.acs.org.

CM0311224